PHYSICAL REVIEW B **70**, 121304(R) (2004)

Defect-induced perturbation on Si(111)4×1-In: Period-doubling modulation and its origin

Geunseop Lee,[1,*] Sang-Yong Yu,[2] Hanchul Kim,[2] and Ja-Yong Koo[2]
[1]*Inha University, Inchon 402-751, Korea*
[2]*Korea Research Institute of Standards and Science, P.O. Box 102, Yuseong, Daejeon 305-600, Korea*
(Received 21 June 2004; published 14 September 2004)

A one-dimensional defect-induced local period-doubling (×2) modulation was observed with scanning tunneling microscopy on a Si(111)4×1-In surface at room temperature. The ×2 modulated region remains metallic in contrast to the low-temperature 4×2 ground-state phase. First-principles calculations predict the lowest-energy state with exactly the same features as observed by H adsorption, but fundamentally different from the experimentally observed insulating ground state at low temperature. This suggests that the true ground state (i.e., the low-temperature phase) is not a band insulator, and is stabilized by many-body interaction.

DOI: 10.1103/PhysRevB.70.121304 PACS number(s): 68.35.−p, 68.37.Ef, 68.43.Bc

Systems with reduced dimensionality frequently show phenomena that may not be present in the related three-dimensional systems due to the change in interactions. One of the examples is a Peierls instability in one-dimensional (1D) system, driven by a perfect Fermi nesting and a large electron-phonon coupling.[1] A Mott insulator may be realized when an electron-electron interaction becomes strong compared with the kinetic energy, which decreases with reduced dimensionality.[2] In recent years, a number of surface systems have attracted considerable attention by exhibiting such phenomena.[3–8]

The role of defects become more important as the dimensionality is reduced.[9] Defects not only create local structural changes, but also affect the phase transition by suppressing the fluctuations that are larger in lower dimensions. In doing so, the defects usually stabilize or mimic the low-temperature (LT) phase in their vicinity at temperatures higher than the transition temperature. Examples include, a defect-induced dimer buckling on Si(100)2×1 at room temperature (RT),[10–12] and defects in Sn/Ge(111)$\sqrt{3}\times\sqrt{3}$ mediating the condensation of the LT 3×3 phase.[13–15] Recently an example emerged for the In/Si(111) with 1 ML of In. While the system undergoes a phase transition from a metallic 4×1 at RT to an insulating 4×2 or 8×2 phase (we will refer to this ground-state LT phase as a GS-4×2 throughout this paper, for simplicity) below 100 K,[3] Na adsorbates were reported to pin the GS-4×2 phase even at RT.[16] For the nature of the GS-4×2, a charge-density wave (CDW) condensate induced by the Peierls instability was proposed,[3] although it was challenged by subsequent studies.[17,18]

In this paper, we report a very different case, where the defect-induced low-symmetry structure differs in nature from the LT phase. On the Si(111)4×1-In surface at RT, highly 1D and period-doubling (×2) modulations in scanning tunneling microscopy (STM) images are observed near a variety of defects. We demonstrate that this defect-induced modulation is metallic and thus not a manifestation of the insulating GS-4×2 phase. This contrasts to the Na adsorption on the same surface. Using density-functional theory (DFT) calculations within the generalized gradient approximation (GGA), the ×2 structural distortion away from the defects has been calculated. These calculations show that a H impurity stabilizes a metallic 4×2 phase, which is the DFT-GGA ground state (GGA-4×2). The GGA-4×2 is fundamentally different from the experimentally observed insulating GS-4×2. This indicates that the stability of the GS-4×2 and its insulating nature need explanation by mechanisms other than the simple Peierls instability inducing CDW.

STM experiments were performed in an ultrahigh vacuum chamber with the base pressure below 1.2×10^{-10} Torr. The preparation of the Si(111)4×1-In surface was described elsewhere.[19] Defects were spotted either by searching for the region on the clean surface or by dosing H_2 and O_2 gases. Gas dosing was done at RT by backfilling the chamber with an ion-gauge filament on for cracking into atoms. The STM measurements were made at RT.

Figure 1 shows RT STM images of the Si(111)4×1-In surface with five different types of defects. The defects

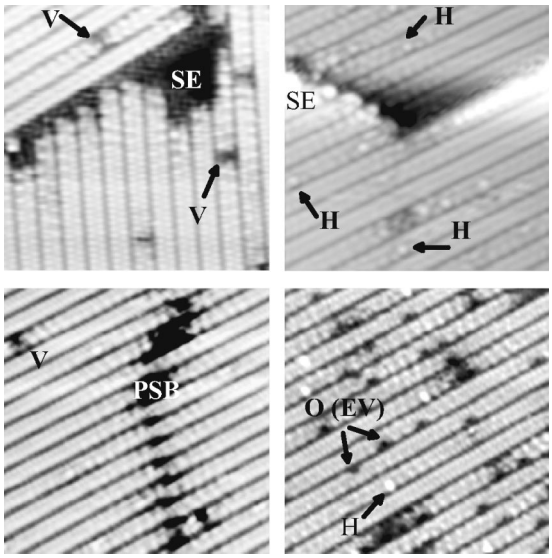

FIG. 1. STM images ($V_s=+0.2$ V, $I_t=0.1$ nA) with various types of defects: vacancy (V), step edge (SE), hydrogen adsorption (H), phase-shift boundary (PSB), and oxygen adsorption (O) or edge vacancy created by oxygen-induced etching (EV). Regardless of the defect types, there are ×2 modulations in the vicinity of defects.

 ©2004 The American Physical Society

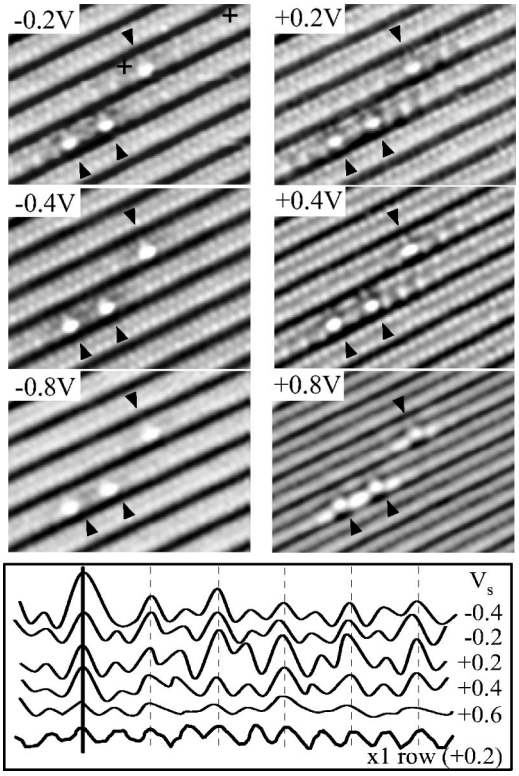

FIG. 2. (top) STM images of the same region showing the bias-voltage dependence near H adsorbates indicated by arrow heads. (bottom) Line scans between two crosses in the −0.2 V image. The position next to H and the ×2 distances are marked by a solid line and dashed lines, respectively.

shown in Fig. 1 are a vacancy, a step edge of an island (or stepped terraces), a phase boundary on a single terrace, H atom adsorption, and O atom adsorption. All these defects induce a ×2 modulation near the defects, superimposed with the atomic corrugation in STM images. The perturbation induced by the defects is highly 1D (we will discuss it later). The amplitude of the modulation decays with distance along the row from the defect, extending up to 10–12 lattice units. This range is much longer than those of the quasi-two-dimensional Sn/Ge(111) and Si(100) cases observed at RT. This also reflects the 1D nature of this perturbation.

STM images of the Si(111)4×1-In surface containing H adsorbates taken at various bias voltages are shown in Fig. 2. The characteristic bias-dependent STM features of the defect-free 4×1 are the same as those previously reported.[19] The modulation near the defects is prominent at low bias voltages. With increasing bias voltage of both polarities, the modulation becomes weaker. Diminution of the ×2 modulation is faster for the filled states ($V_s<0$ V) than for the empty states ($V_s>0$ V). This bias-voltage dependence of the modulation observed for the H adsorbate is representative, and shared by all other defects presented in Fig. 1. Differently from the modulation amplitude, the period of the modulation (×2) does not depend on the bias as shown in the bottom panel of Fig. 2. It is noted that the appearance of the ×2 modulation is quite different from those reported for the GS-4×2 phase[3] and the Na-induced ×2 modulation.[16]

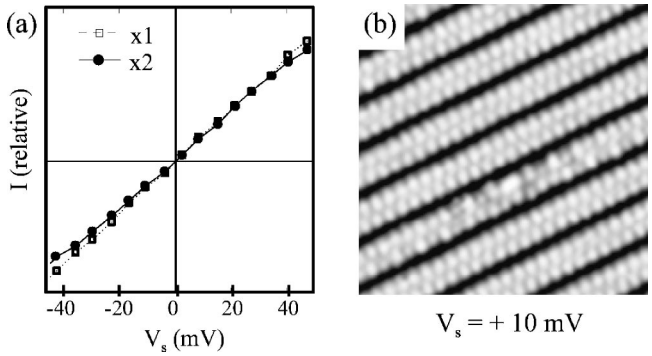

FIG. 3. (a) *I-V* data measured at points of unperturbed ×1 and perturbed ×2 rows. (b) An STM image acquired with $V_s=+10$ mV and $I_t=0.17$ nA.

The defect-induced modulation in the STM images of the Si(111)4×1-In surface appear quite similar to those of the electron screening reported in a number of surfaces.[20] The metallic Si(111)4×1-In surface has three surface-state bands crossing the Fermi level, one of which has a Fermi wave vector of $k_F\sim G_0/2$, with G_0 being the zone boundary in the row (×1) direction.[3,18] The observed ×2 modulation period is apparently consistent with the wavelength of the electron screening corresponding to this k_F. It is noted that the wavelength of the electron standing wave is to be energy dependent.[21] The observed bias independency of the modulation period is incompatible with a simple electron standing wave picture of screening, and requires a consideration which goes beyond a simple plane-wave response. The lattice response to the electron screening must be included.

If the lattice response is important, the obvious possibility for the origin of the defect-induced modulation is the local manifestation of the GS-4×2 phase. The GS-4×2 phase was reported to have a significant lattice distortion from the 4×1 structure as determined by a surface x-ray diffraction (SXRD).[17] Previously, Na adsorption was reported to induce this GS-4×2 at RT, based on close similarities in spectroscopic data and in STM appearance.[16] For both the GS-4×2 and the Na-induced ×2 phase at RT, the existing electron spectroscopy data show a band gap or significant reduction in density of states (DOS) at E_F, $N(E_F)$.[3,16,22] However, the case of the defects in our study is different. The ×2 modulated region in our case remains metallic in contrast to the gap opening (0.1–0.15 eV) reported in the Na case. This is clearly demonstrated in the current-voltage (*I-V*) characteristics near zero bias in Fig. 3(a). There is virtually no reduction in $N(E_F)$. Stable STM imaging of the ×2 area was even possible at a bias as low as ±0.01 V [see Fig. 3(b)], which is well within the band gap of the Na-induced phase even considering the thermal energy of RT (~0.025 eV). Therefore, we infer that the defect-induced ×2 modulation observed in this work is different from the GS-4×2. The dissimilar appearances in the STM images also support their difference. Figure 3(b) also clearly shows that the defect-induced perturbation is highly 1D, being confined only in the row where the defect is located.

We have performed *ab initio* pseudopotential calculations within DFT-GGA.[23] First, we calculated the electronic band

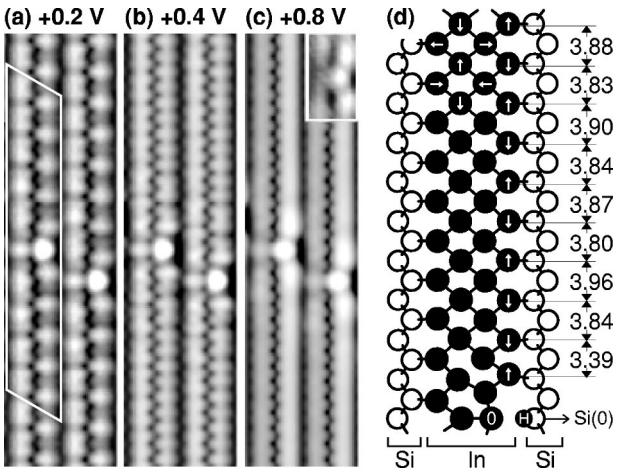

FIG. 4. (a)–(c) Simulated STM images of the 4×1-In surface with an H adsorbate in the 4×21 supercell (parallelogram). The inset in (c) is the experimental counterpart of the H adsorbate. (d) Relaxed geometry around the H atom. A schematic in-plane relaxation pattern is represented by arrows. The interatomic distances between In atoms projected on the row direction is designated in Å. The projected inter-In distance is 3.86 Å for the unperturbed 4×1 surface.

structure of the GS-4×2 phase. Although the structure of the GS-4×2 phase is not fully established, we referred to the existing SXRD data of the lattice structure.[17] Without relaxation, our calculations did not find either a gap opening or significant reduction in $N(E_F)$, agreeing with a previous calculation.[18] With relaxation, we found a new lowest-energy 4×2 structure (GGA-4×2) that is still metallic. The GGA-4×2 possesses a slight lattice distortion from the 4×1, differentiating from the observed GS-4×2 phase. This newly found GGA-4×2 differs from the RT-4×1 and the previously calculated 4×2,[18] too. The discrepancy with the experiments[3,22] is an indication that the ground-state GS-4×2 phase is not a simple band insulator.

We now turn to the case with defects to elucidate the origin of the observed defect-induced modulation. H atom adsorption was chosen as a test case that is simple and tractable. H atoms are found to be preferably inserted into In-Si bonds on the surface layer. We adopted a 4×21 supercell (21 lattice units along the row) to simulate the *isolated* H adsorption. While detailed theoretical results will be presented elsewhere,[24] the simulated STM images are shown in Fig. 4 with the relaxed atomic geometry. The agreement between the theoretical and experimental images (Fig. 2) is remarkable. The simulations reproduce not only the characteristic H feature, but also the ×2 modulation of the In chains along the row, the bias dependence of the modulation, and the observed *I-V* characteristics.[25] The fast disappearance of the modulation with increasing bias voltages indicates that the defect-induced perturbation in the electronic charge profile (that is, local DOS) is mainly concentrated in the states near E_F. However, the change in $N(E_F)$ is not significant.

Upon adsorption, an H atom breaks one of the surface In-Si bonds and forms a Si-H bond [Si(0)-H in Fig. 4(d)], making the reacted In atom [In(0) in Fig. 4(d)] significantly displaced from the unperturbed position. This perturbation propagates far enough to induce structural modification in the region away from the defect site. According to our calculations, the structural modification is present throughout the whole 4×21 cell, consistent with the observed perturbation range of up to ten ×1 lattice units from the H adsorbate on the row. The structural change at locations away from the H atom is characterized by the pattern shown in Fig. 4(d). This lattice distortion takes a symmetry of the normal mode at the zone boundary of 4×1 structure. Distant from the H adsorbate in our 4×21 supercell, the magnitude of the atomic displacement is only about ~0.03 Å. This is an order of magnitude smaller compared with both the SXRD (0.65 Å)[17] and the previous calculation by Cho *et al.* (0.28 Å).[18]

Based on the same appearance of the observed ×2 modulations for a variety of defects and their resemblance to the GGA-4×2 geometry, it is inferred that the defect-induced 4×2 modulation commonly adopts the 4×2 geometry of the defect-free surface, GGA-4×2. This 4×2 geometry is nearly degenerate with the 4×1 (the energy lowering is only about ~1 meV/4×1, well within the accuracy of DFT calculations). Due to the negligible energy difference found in our calculations, it is difficult to tell which one is the lowest-energy state in the framework of the DFT-GGA.[26] However, it is plausible that the presence of defects may tilt the energy balance. We believe that this happens on the Si(111)-In surface. The defects stabilize the GGA-4×2 geometry in their vicinity, inducing the ×2 modulation on the 4×1-In surface at RT.

In many surfaces showing the temperature-driven structural phase transition, a symmetry breaking defect locally stabilizes the LT phase or eventually leads to it via interference with other defects, at temperatures above T_c. Such examples include the *C* defect or C_2H_2 on Si(100),[11,12] the vacancy or Ge-substitutional defects in Sn/Ge(111),[14] and the Na adsorbate on In/Si(111)-4×1.[16] Contrasting with these examples, our work constitutes an exceptional case, where the local reduced-symmetry structure does not take that of the LT phase.

Our findings and the inferences drawn from the comparison with past studies can be summarized as (1) *There are two different 4×2 structures*: *GS-4×2 and GGA-4×2*. The GS-4×2 is an experimentally observed LT phase having large lattice distortion. While this was proposed to be a CDW condensate based on the Fermi nesting observed in the photoemission spectroscopy data,[3] the calculations cast some doubts on the origin of its insulating property. The GGA-4×2 is the lowest-energy state found in the present set of DFT calculations, for which the slight energy lowering is achieved through the charge redistribution accompanying the weak ×2 lattice distortion. (2) *Defects (studied in this work) on the 4×1 surface at RT stabilize the GGA-4×2 structure predicted by the DFT-GGA theory*. It is obvious from this work that the GGA-4×2 state which is stabilized by our defects is different from the GS-4×2 LT phase. This is an unusual observation, indicating that the phase diagram of this system could be more complex than anticipated.

An intriguing but hypothesized scenario for the temperature-driven phase transition of the defect-free surface and the influence of the defects is proposed. At RT, the sur-

face has a 4×1 structure seen by low-energy electron diffraction (LEED) and STM. Upon cooling, the RT-4×1 phase becomes subject to a structural phase transition into a low-symmetry phase. The DFT calculations predict an *order-disorder* transition to the GGA-4×2 structure, where the dynamical fluctuation is suppressed. However, it seems that a *third* phase (the true ground-state GS-4×2) starts to develop around T_c. Thus, in reality, the temperature-driven phase transition becomes a *displacive* type. The GS-4×2 phase has a structural distortion much larger than the GGA-4×2, and is insulating. Although it is likely that the structural distortion is driven by Peierls instability, the insulating property is not compatible with a simple Peierls CDW picture as previously proposed[3] and needs an explanation which goes beyond it. At RT, the role of defects in our study is to stabilize the DFT-predicted GGA-4×2 structure.

At present, the reason why different defects (the defects in our work and Na) stabilize different phases (GGA-4×2 predicted in theory and ground-state GS-4×2, respectively) at RT is unknown. Further work is needed to unveil the mechanisms behind this difference.

This work was supported by MOST of Korea through "The National R&D Project for Nano Science and Technology" and "The Creative Research Initiative," and partly by Grant No. R02-2004-000-10262-0 from the Basic Research Program of the Korea Science and Engineering Foundation. H.K. acknowledges support from the KISTI under "The Fifth Strategic Supercomputing Support Program."

*Author to whom correspondence should be addressed. Electronic mail: glee@inha.ac.kr

[1] R. E. Peierls, *Quantum Theory of Solids* (Clarendon, Oxford, 1964).

[2] N. F. Mott, *Metal-Insulator Transitions*, 2nd ed. (Taylor and Francis, New York, 1990).

[3] H. W. Yeom, S. Takeda, E. Rotenberg, I. Matsuda, K. Horikoshi, J. Schaefer, C. M. Lee, S. D. Kevan, T. Ohta, T. Nagao, and S. Hasegawa, Phys. Rev. Lett. **82**, 4898 (1999).

[4] T. Nakagawa, G. I. Boishin, H. Fujioka, H. W. Yeom, I. Matsuda, N. Takagi, M. Nishijima, and T. Aruga1, Phys. Rev. Lett. **86**, 854 (2001).

[5] K. Swamy, A. Menzel, R. Beer, and E. Bertel, Phys. Rev. Lett. **86**, 1299 (2001).

[6] J. M. Carpinelli, H. H. Weitering, E. W. Plummer, and R. Stumpf, Nature (London) **381**, 398 (1996).

[7] N. J. DiNardo, T. M. Wong, and E. W. Plummer, Phys. Rev. Lett. **65**, 2177 (1990).

[8] H. H. Weitering, X. Shi, P. D. Johnson, J. Chen, N. J. DiNardo, and K. Kempa, Phys. Rev. Lett. **78**, 1331 (1997).

[9] D. R. Nelson, *Phase Transitions and Critical Phenomena*, edited by C. Domb and J. L. Lebowitz (Academic, London, 1983), Vol. 7,1.

[10] R. M. Tromp, R. J. Hamers, and J. E. Demuth, Phys. Rev. Lett. **55**, 1303 (1985).

[11] R. J. Hamers and U. K. Kohler, J. Vac. Sci. Technol. A **7**, 2854 (1989).

[12] W. Kim, H. Kim, G. Lee, Y.-K. Hong, K. Lee, C. Hwang, D.-H. Kim, and J.-Y. Koo, Phys. Rev. B **64**, 193313 (2001).

[13] H. H. Weitering, J. M. Carpinelli, A. V. Melechko, J. Zhang, M. Bartkowiak, and E. W. Plummer, Science **285**, 2107 (1999).

[14] A. V. Melechko, J. Braun, H. H. Weitering, and E. W. Plummer, Phys. Rev. Lett. **83**, 999 (1999).

[15] T. E. Kidd, T. Miller, M. Y. Chou, and T.-C. Chiang, Phys. Rev. Lett. **85**, 3684 (2000).

[16] S. S. Lee, J. R. Ahn, N. D. Kim, J. H. Min, C. G. Hwang, J. W. Chung, H. W. Yeom, S. V. Ryjkov, and S. Hasegawa, Phys. Rev. Lett. **88**, 196401 (2002).

[17] C. Kumpf, O. Bunk, J. H. Zeysing, Y. Su, M. Nielsen, R. L. Johnson, R. Feidenhans'l, and K. Bechgaard, Phys. Rev. Lett. **85**, 4916 (2000).

[18] J.-H. Cho, D.-H. Oh, K. S. Kim, and L. Kleinman, Phys. Rev. B **64**, 235302 (2001).

[19] G. Lee, S.-Y. Yu, H. Kim, J.-Y. Koo, H.-I. Lee, and D. W. Moon, Phys. Rev. B **67**, 035327 (2003).

[20] M. F. Crommie, C. P. Lutz, and D. M. Eigler, Nature (London) **363**, 524 (1993); Y. Hasegawa, and Ph. Avouris, Phys. Rev. Lett. **71**, 1071 (1993); P. T. Sprunger, L. Petersen, E. W. Plummer, E. Lægsgaard, and F. Besenbacher, Science **275**, 1764 (1997).

[21] The bias-dependent modulation wavelength can appear not only in dI/dV images but also in topographic images, especially for empty-state bias, where the tunneling is most weighed to the highest states of the applied voltage. Refer to an example [T. Yokoyama, M. Okamoto, and K. Takayanagi, Phys. Rev. Lett. **81**, 3423 (1998)].

[22] H. W. Yeom, K. Horikoshi, H. M. Zhang, K. Ono, and R. I. G. Uhrberg, Phys. Rev. B **65**, 241307 (2002).

[23] G. Kresse and J. Furthmüller, Phys. Rev. B **54**, 11 169 (1996).

[24] H. Kim (unpublished).

[25] Calculations using a 8×9 supercell show that the perturbation is confined only along the row without affecting the neighboring rows, confirming the experimental finding.

[26] In our calculations, the DFT-GGA geometry reported by Cho *et al.* (Ref. 18) has a higher energy than the GGA-4×2 by about 20 meV/4×1, and is unstable.